Journal of Alloys and Compounds 483 (2009) 102–106

Contents lists available at ScienceDirect

Journal of Alloys and Compounds

journal homepage: www.elsevier.com/locate/jallcom

Evaluation of glass-forming ability of binary metallic glasses with liquidus temperature, crystallographic data from binary phase diagrams and molecular dynamics simulations

A. Takeuchi*, K. Yubuta, A. Makino, A. Inoue

Institute for Materials Research, Tohoku University, Sendai 980-8577, Japan

ARTICLE INFO

Article history:
Received 30 August 2007
Received in revised form 5 July 2008
Accepted 15 July 2008
Available online 12 December 2008

Keywords:
Amorphous materials
Clusters
Intermetallics
Disordered systems
Crystal structure and symmetry

ABSTRACT

The glass-forming ability (GFA) of binary metallic glasses was analyzed with data for the liquidus temperature (T_l) acquired as a function of composition from binary phase diagrams, assisted by crystallographic data combined with amorphous-forming composition range (AFCR) and molecular dynamics (MD) simulations. A necessary condition for the formation of bulk metallic glasses (BMGs) was determined as $\Delta T_l \geq 300$ K where ΔT_l was defined as a decrease in T_l due to eutectic reaction. The crystalline compounds with structure types of bcc or its derivative type, such as CsCl (B2), CrB (B_f), Al_2Cu (C16) and $MoSi_2$ ($C11_b$), tended to be found in AFCR frequently. The total pair-distribution and interference functions revealed a high forming tendency of a noncrystalline $Cu_{10}Zr_7$ structure created by MD. Simultaneous achievements of the $Cu_{10}Zr_7$ structure for crystallographic features resulting from the bcc family structure and geometrical features in phase diagram for T_l affect the formation of $Cu_{61.8}Zr_{38.2}$ BMG.

1. Introduction

Recently, several bulk metallic glasses (BMGs) have been fabricated in binary systems, such as Cu–Zr [1–3], Cu–Hf [1,4,5], Ni–Nb [6] and Ca–Al [7] systems. These binary BMGs provide advantage over multicomponent BMGs [8] for their fabrication, analysis and so on because of the relative simplicity in the number of constituent elements. Accordingly, it is worth reviewing the possibility to fabricate BMGs in every possible binary system by referring to a series of important findings of binary noncrystalline alloys carried out in 1980s or before, such as eutectic reaction in phase diagrams. For instance, it was reported [9] that noncrystalline alloys can be formed in a system with deep eutectic reaction in a phase diagram when the alloys are rapidly quenched from a liquid. The deep eutectic would indicate a steep or considerable decrease in liquidus temperature (T_l) in a composition range. To the authors' knowledge, however, quantitative analyses concerning the deepness of the eutectic reactions have not yet been carried out to date. In addition, the relationships between a eutectic reaction and crystallographic features of compounds involved in the eutectic reaction remains also uncertain.

The present study aims to perform quantitative analysis of the glass-forming ability (GFA) in binary systems with parameters derived from T_l acquired from binary phase diagrams, and to clarify the relationships between the formation of binary BMGs and the crystallographic features of binary compounds with respect to local atomic arrangements.

2. Methods

Database for T_l in A–B binary alloy systems has been created as a function of composition (c_B) at a composition interval (Δc_B) of 0.1 at% of B element. The 2057 binary systems from binary phase diagrams [10] and crystallographic data of 9082 binary compounds were dealt with in the database. The numerical values of T_l were obtained by digitization of the phase diagrams with software and the values were summarized with another piece of commercial software. In addition, amorphous-forming composition range (AFCR) for 81 binary systems was also digitized from the literature [11]. These numerical values in the database were regarded as primary data, and were used for evaluating the following parameters: (1) changes in T_l due to eutectic reaction and (2) the first- and second-order derivatives of T_l with respect to c_B, (dT_l/dc_B and d^2T_l/dc_B^2), which were evaluated by difference method at each composition interval of 0.5 at%.

In evaluating the changes in T_l due to a eutectic reaction, we paid attention to the types of melting of compounds: congruent melting, pertectic reaction type, or others. In particular, the compounds that exhibit congruent melting were focused on because they have a possibility to be involved in a eutectic reaction. The congruent melting type compounds in eutectic reaction were determined empirically by evaluating temperature interval due to the decrease in T_l ($\Delta T_1 = \sum c_i T_m^i - T_1$) where $\sum c_i T_m^i$ (i = A, B) is defined by the melting temperature of pure elements (T_m^A and T_m^B).

* Corresponding author at: Katahira 2-1-1, Aoba-ku, Sendai 980-8577, Japan. Tel.: +81 22 215 2112; fax: +81 22 215 2111.
E-mail address: takeuchi@imr.tohoku.ac.jp (A. Takeuchi).

0925-8388/$ – see front matter © 2008 Elsevier B.V. All rights reserved.
doi:10.1016/j.jallcom.2008.07.186

Table 1
Crystallographic data for the $Ni_{10}Zr_7$ structure (Pearson symbol: oC68; space group: *Aba2*; lattice constants: $a = 0.9211$ nm, $b = 0.9156$ nm, $c = 1.2386$ nm). MWl is Multiplicity Wyckoff letter.

Number	Atom	MWl	*x*	*y*	*z*	Occupancy
1	Zr1	4 a	0	0	.9545	1
2	Zr2	4 a	0	0	.6434	1
3	Zr3	4 c	0	0	.2572	1
4	Ni1	8 b	.2100	.0008	.7582	1
5	Ni2	8 b	.2915	.0082	.5956	1
6	Ni3	8 b	.0031	.2919	.5978	1
7	Ni4	8 b	.0122	.2986	.3082	1
8	Ni5	8 b	.1063	.1090	.4501	1
9	Zr4	8 b	.2459	.2560	.7018	1
10	Zr5	8 b	.3129	.3106	.4529	1

The MD simulations were also performed for $Cu_{10}Zr_7$ structure. The prototype of the $Cu_{10}Zr_7$ is the $Ni_{10}Zr_7$ structure, the crystallographic features of which are summarized in Table 1. The $Cu_{10}Zr_7$ structure was selected because of success in forming $Cu_{61.8}Zr_{38.2}$ BMG [2], the composition of which is close to the $Cu_{10}Zr_7$ compound ($Cu_{58.8}Zr_{41.2}$). The $Cu_{10}Zr_7$ structure was obtained by substituting Ni atoms with Cu from the $Ni_{10}Zr_7$ structure, and by applying the lattice constants of $Cu_{10}Zr_7$: $a = 0.9347$ nm, $b = 0.9313$ nm and $c = 1.2675$ nm [12]. The MD simulations performed for the $Cu_{10}Zr_7$ structure was based on a method used in our previous studies for the analysis of local atomic arrangements of C_6Cr_{23} structure [13] and metastable Zr_2Ni structure [14]. A feature of this method includes a scheme to treat groups of atoms as clusters in a crystalline structure [13,14]. In the present study, two types of clusters (Clusters 1 and 2) were taken into account for $Cu_{10}Zr_7$ crystalline structure, which belongs to space group of *Aba*2 (space group number 41) [15]. The Cluster 1 has a shape of distorted polyhedron, which is denoted by coordination number (C.N.) of 14 around a Zr1 atom, as shown in Fig. 1. The Cluster 2 is obtainable from Cluster 1 by applying a symmetry operation of reflection (σ) toward *x*–*z* plane, $\sigma(x,y,z) \rightarrow (x,-y,z)$, for Cluster 1. As a result, the $Cu_{10}Zr_7$ structure can be regarded as an ensemble of Clusters 1 and 2 and remaining Zr4 atoms in Table 1. Cluster 1 occupy the sites at (0, 1/2, .4545) and (0, 0, .9545) while Cluster 2 at (1/2, 0, .4545) and (1/2, 1/2, .9545), and remaining Zr4 atoms are near (1/4, 1/4, .7).

Four structures (Structures 1–4) were dealt with in the MD simulations for $Cu_{10}Zr_7$ alloy. Structure 1 was exactly the same to the crystalline $Cu_{10}Zr_7$ structure while Structure 2 with atomic bonds for clusters corresponded to the Structure 1. Structure 3 was obtained by allowing random rotations of clusters around their center of mass for Eulerian angle from 0 to 360° in Structure 2. After releasing atomic bonds for the clusters, Structure 4 was created from Structure 3 by applying low-temperature annealing (500 K, 4 ps) with Generalized Embedded Atom Method (GEAM) potential under a periodic boundary condition and the number of atoms, temperature, and volume (constant-NTV) conditions. The MD simulations were performed for the $3 \times 3 \times 3$ supercell of the $Cu_{10}Zr_7$ structure. The total pair-distribution and total interference functions were evaluated with the commercial MD software.

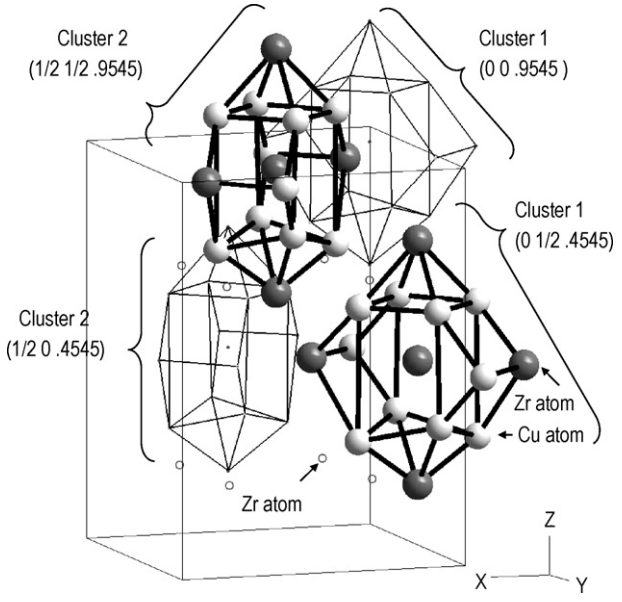

Fig. 1. A ball and skeleton view of the unit cell of the $Cu_{10}Zr_7$ structure drawn with Clusters 1 and 2 and remaining Zr atoms.

3. Results and discussion

The statistical analysis of compounds for 81 binary systems by referring to their AFCR [11] revealed that compounds, which are involved in eutectic reaction, tended to exhibit a relationship expressed by $T_m^{Comp.} / \sum c_i T_m^i \geq 0.85$ where $T_m^{Comp.}$ is the melting temperature of the congruent melting type compound. As shown in Fig. 2, the $Cu_{51}Zr_{14}$ compound in the Cu–Zr binary system is involved in two eutectic reactions, Eutectics (1) and (2), and is the only compound that satisfied the relationship in the intermediate compounds of Cu_9Zr_2, $Cu_{51}Zr_{14}$, Cu_8Zr_3, $C_{10}Zr_7$, CuZr and $CuZr_2$. However, there exists an exception of this tendency in other system than the Cu–Zr system when the compounds are found in AFCR. The details of the exception will be explained in the next paragraph.

The numerical analysis of GFA for 81081 alloy compositions (81 systems at 0.1 at% intervals of c_B) revealed that there exists 159 alloys which satisfy a set of conditions both $|dT_l/dc_B| \geq 100\,K\,at\%^{-1}$ and $\Delta T_l \geq 100\,K$. The 159 alloys include $Fe_{24}Zr_{76}$ and $Os_{43.9}Zr_{56.1}$, which posses the largest values of $|dT_l/dc_B|$ and ΔT_l, although they

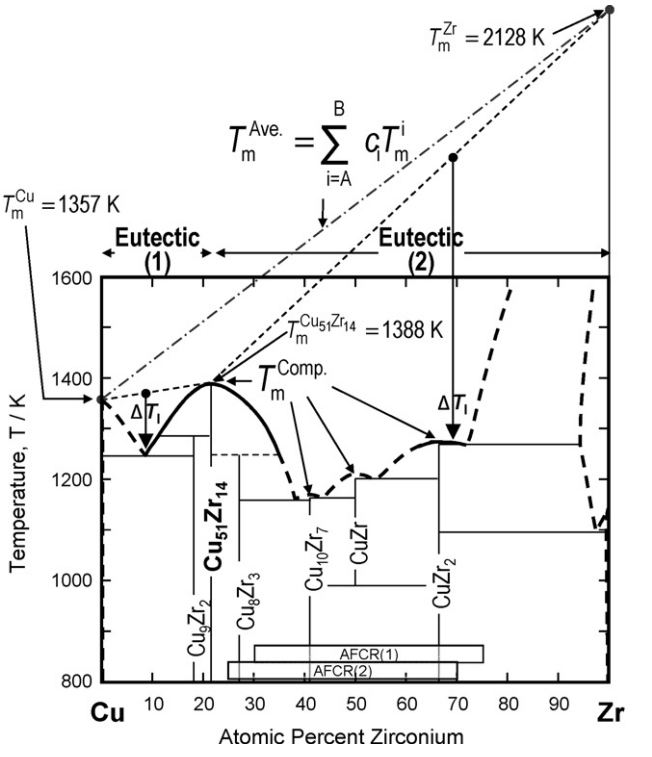

Fig. 2. The Cu–Zr binary phase diagram in which the method to determine the intermediate compounds involved in eutectic reactions. The AFCRs were acquired from the literature [11].